Structure of boron carbide under laser-based shock-compression at 51 GPa

Cite as: AIP Conference Proceedings **2272**, 100010 (2020); https://doi.org/10.1063/12.0000846
Published Online: 04 November 2020

B. Glam, S. J. Tracy, R. F. Smith, J. K. Wicks, D. E. Fratanduono, A. E. Gleason, C. A. Bolme, V. B. Prakapenka, S. Speziale, K. Appel, H. J. Lee, A. Mac Kinnon, F. Tavella, J. H. Eggert, and T. S. Duffy

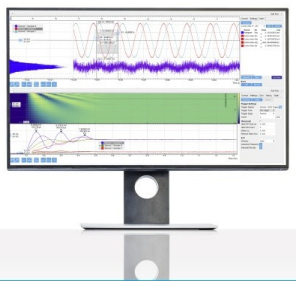

Structure of Boron Carbide Under Laser-Based Shock-Compression at 51 GPa

B. Glam[1, a)], S. J. Tracy[2, 3], R. F. Smith[4], J. K. Wicks[2, 5], D. E. Fratanduono[4], A. E. Gleason[6], C. A. Bolme[7], V. B. Prakapenka[8], S. Speziale[9], K. Appel[10], H. J. Lee[11], A. MacKinnon[11], F. Tavella[11], J. H. Eggert[4], and T. S. Duffy[2]

[1]*Dept. of Applied Physics, Soreq NRC, Yavne, 81800, Israel*
[2]*Dept. of Geosciences, Princeton University, Princeton, NJ, 08544, USA*
[3]*Now at Geophysical Laboratory, Carnegie Institution for Science, USA*
[4]*Physics Division, Lawrence Livermore National Laboratory, Livermore, CA, 94550, USA*
[5]*Now at Department of Earth and Planetary Sciences, Johns Hopkins University, Baltimore, Maryland 21218 USA*
[6]*Stanford Institute for Materials and Energy Sciences, SLAC National Accelerator Laboratory, Menlo Park, California 94025 USA*
[7]*Shock and Detonation Physics, Los Alamos National Laboratory, Los Alamos, New Mexico 87545 USA*
[8]*GeoSoilEnviroCARS University of Chicago, Argonne National Laboratory, Argonne, Illinois 60439 USA*
[9]*GFZ German Research Centre for Geosciences, Telegrafenberg, 14473 Potsdam*, Germany
[10]*European XFEL GmbH, Holzkoppel 4, D-22869 Schenefeld, Germany*
[11]*Linac Coherent Light Source, SLAC National Accelerator Laboratory, Menlo Park, California 94025 USA*

[a)]Corresponding author: benny.glam@gmail.com

Abstract. *In situ* x-ray diffraction and wave-profile measurements were carried out on polycrystalline boron carbide under laser-induced shock compression at 51 GPa at the Matter in Extreme Conditions end-station of the Linac Coherent Light Source. The diffraction data indicate that boron carbide remains crystalline to this pressure and there is no evidence for a major structural phase transition. The peak elastic stress for boron carbide was found to be 15.9 GPa, in agreement with previous gas-gun measurements, despite differences in sample thickness and loading rate between laser and gas-gun compression. The starting sample contained excess carbon in the form of graphite. The graphite peaks disappeared upon compression of the sample, indicating that carbon was incorporated into the structure of boron carbide behind the shock front and retained upon decompression.

INTRODUCTION

Boron carbide is widely used as a high-strength, low-density constituent of armor due to its exceptional hardness, thermodynamic stability, and electronic properties [1]. The building blocks of boron carbide are a B_{12} icosahedron with electron deficient B-B bonds (δ bond) [2] and a triatomic linker unit that bonds neighboring icosahedra [3]. Shock-wave experiments using continuum velocity measurements show loss of strength above the elastic limit. Kinks in the shock velocity-particle velocity curve and Hugoniot pressure-density at 20-40 GPa and above 40 GPa are associated with pressure-induced volume collapses [4]. At present, it is unclear if the loss of strength is related to localized amorphization or a polymorphic phase transition [5]. In this work, *in situ* x-ray diffraction and continuum velocity measurements in shock-compressed boron carbide at 51 GPa are presented.

Shock Compression of Condensed Matter - 2019
AIP Conf. Proc. 2272, 100010-1–100010-6; https://doi.org/10.1063/12.0000846
Published by AIP Publishing. 978-0-7354-4000-5/$30.00

EXPERIMENTAL SETUP

Dynamic compression experiments were carried out at the Matter in Extreme Conditions (MEC) end-station [6] at the Linac Coherent Light Source (LCLS) of the Stanford Linear Accelerator Center (SLAC). Polycrystalline boron carbide samples (nominally B_4C) were obtained from Insaco Inc., the same supplier used in another recent shock compression study [7]. Ambient X-ray diffraction revealed a spotty pattern with grain size estimated to be ~10 µm. The observed diffraction peaks can be assigned either to rhombohedral (R-3m) boron carbide or excess carbon in the form of graphite inclusions. The average lattice parameters of boron carbide were determined to be a= 5.61±0.02 Å and c= 12.10±0.02 Å. It should be noted that boron carbides can exhibit variable carbon contents due to substitution between B and C at icosahedral and chain lattice sites and the presence of vacancies. Our boron carbide samples appear to be slightly carbon deficient relative to B_4C.

The samples were cut and polished to dimensions of 1.5 x 1.5 x 0.060 mm and glued to polyimide (CH) ablators (~75-µm thick) with a thin epoxy layer. In some cases, (100) LiF windows (100-µm thick) were attached to the rear surface of the samples. An Al coating was deposited on the LiF window at the sample/LiF interface. The samples were dynamically compressed using ~10 J pulses from a 527-nm Nd:Glass laser system [8] focused to a diameter of 250 µm. The laser pulses were 10-ns long with a quasi-flat-top shape. A line-focused VISAR [6] (velocity interferometer system for any reflector) was used to monitor either the free surface velocity or the velocity at the sample-window interface. Samples were probed with ~0.1455 nm (~8.52 keV) free electron laser x-rays focused to ~40 µm in diameter. Diffracted X-rays were recorded using in-vacuum integrating pixel array detectors (CSPads) [9] as shown in Fig. 1. A series of shots was performed on nominally identical targets using the same drive conditions but different time delays between the laser and X-ray pulses. Here we describe a subset of these experiments focusing on nearly fully compressed and released states.

.

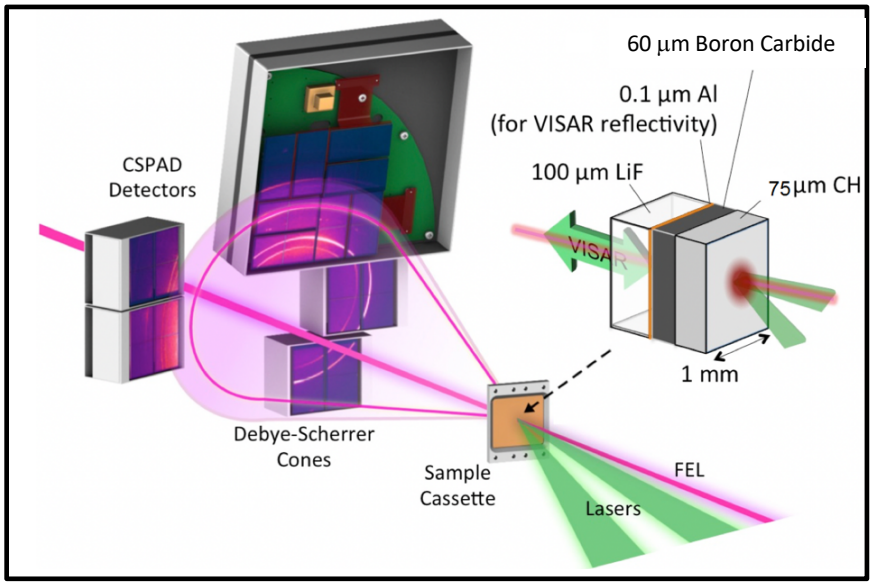

FIGURE 1. Schematic of the experimental setup. The LCLS x-ray beam was incident at 15 degrees to target normal and the two nanosecond laser arms were oriented at 6 and 25 degrees. Diffracted X rays were recorded on CSPAD detectors. The target package (right) shows the CH ablator, boron carbide sample, and LiF window. The VISAR was focused on the LiF-sample interface or sample free surface.

EXPERIMENTAL RESULTS

VISAR continuum results

Representative velocity profiles measured by VISAR at the free surface and sample-LiF window interface are shown in Fig. 2. The profiles show a two-wave structure that we interpret as an initial elastic wave followed by a

slower plastic wave. The wave profiles show some velocity irregularities that may reflect heterogeneous deformation of the sample as previously reported in gas-gun experiments [10]. The pressure at the shock-compressed state was determined from the measured sample-LiF interface velocity using impedance matching with the known equation of state of LiF and the density (2.88 g/cm^3) of boron carbide measured by x-ray diffraction (described below). The difference between longitudinal stress and hydrostatic pressure was not included here. The elastic limit appears as the first change in the free-surface velocity slope in Fig. 2. Consistent with previous work [11, 12], our wave profiles do not exhibit additional step-like features often observed in the case of phase transitions. The peak elastic stress was found to be 15.9 GPa and the corresponding density obtained from the velocity measured by VISAR at this stress is 2.59 g/cm^3. These results are in a good agreement with previous continuum measurements of the Hugoniot Elastic Limit (15–18 GPa) in gas gun experiments [11]. The samples in our study are significantly thinner than those used in plate impact experiments [11, 12, 13], 0.06 mm versus 2.3-9.6 mm, respectively, revealing no evidence for elastic precursor decay or strain-rate dependence. It is interesting to compare this behavior to other materials, in particular the lightweight ceramic SiC, where elastic limit enhancement was found in high-strain rate laser-drive experiments [14]. Previous studies found that the compressive failure threshold of SiC is characterized by transition from brittle to ductile while boron carbide remains brittle [15]. This might explain our finding for non-elastic precursor decay or strain rate dependence in boron carbide since elastic precursor enhancement may be related to dislocations in ductile materials.

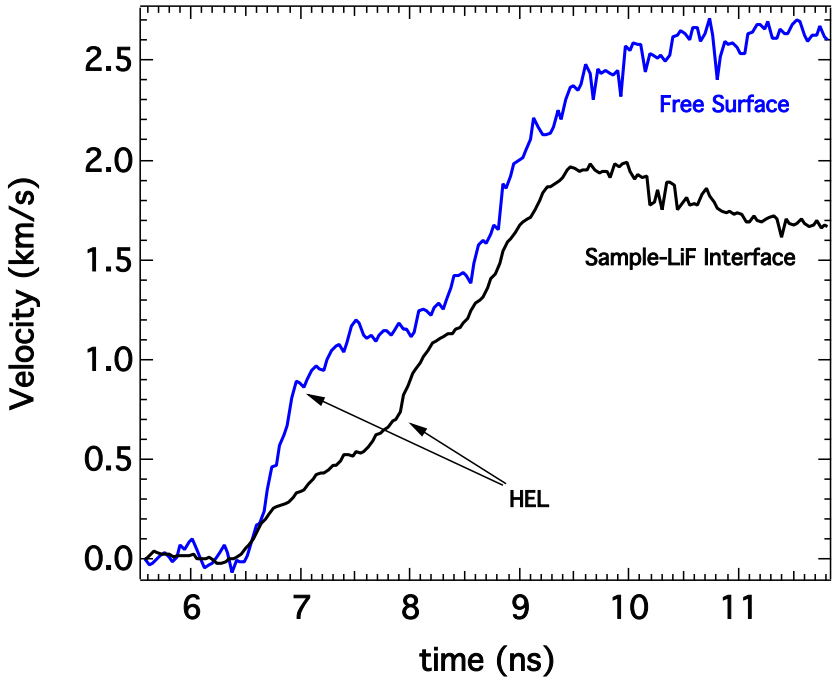

FIGURE 2. Representative velocity profiles measured by VISAR at the free surface (blue) and sample-LiF window interface (black). The first jump in the velocity profile represents the elastic wave arrival at the free surface or sample-LiF window interface.

In-situ x-ray diffraction results

A two-dimensional X-ray diffraction image for shock compressed boron carbide at ~51 GPa is shown in Fig. 3. The image is complex and includes diffraction from three states: 1) uncompressed 2) elastically compressed and 3) plastically compressed material. The pattern consists of a combination of bright spots together with elongated and diffuse features, indicating that large crystallites are retained and the strain distribution is heterogeneous. Figure 4 shows selected integrated one-dimensional diffraction patterns for the pre-shot state, compression to ~51 GPa and the

release state at late time. The X-ray probe delay time (relative to laser turn-on) and the densities calculated from the diffraction data are shown to the right of each pattern. The peaks in the pre-shot pattern can be assigned to rhombohedral boron carbide except for a peak near 3.35 Å assigned to the (002) reflection of graphite inclusions.

In the shock-compressed pattern, a subset of the diffraction spots can be identified as arising from elastic compression of the sample (Fig. 4). Fitting these peaks to a hexagonal unit cell yields the parameters: a=5.51±0.02 Å, c=11.91 ±0.05 Å and V=313.1±0.3 Å^3. The corresponding density is 2.63±0.03 g/cm^3, in the range of HEL values reported in the literature (2.59-2.65 g/cm^3) [11, 12,13] and calculated from our continuum velocity measurements.

Shock compressed peaks in boron carbide can be identified as indicated in Figures 3 and 4, although there can be some overlap with ambient and elastic peaks. All the observed peaks are assigned to reflections from the R-3m structure and there is no evidence for any major phase transformation to this pressure. The unit cell parameters at 51 GPa are: a= 5.38±0.02 Å, c=11.43±0.04 Å and V=286.5±1.9 Å^3. The values are consistent with the results of static diamond anvil cell experiments [16, 17] and the corresponding density (2.88±0.06 g/cm^3), assuming a B_4C composition is consistent with continuum Hugoniot results [11]. The broad, spotty diffraction features observed at this pressure indicate that the sample retains relatively large grains and is subjected to a broad distribution of strains. Note that the carbon peak is not observed in the shock-compressed pattern, suggesting that the carbon was incorporated into the structure of boron carbide behind the shock front. The topmost trace in Fig. 4 shows the diffraction pattern at late time when the sample is largely decompressed. The peaks are sharp and much more ring-like, indicating that the crystallites have broken up during the decompression process. The carbon peak is not seen, suggesting that the carbon has been retained in boron carbide during release. The lattice parameters are slightly expanded relative to the pre-shot due to the combined effects of residual temperature and carbon incorporation.

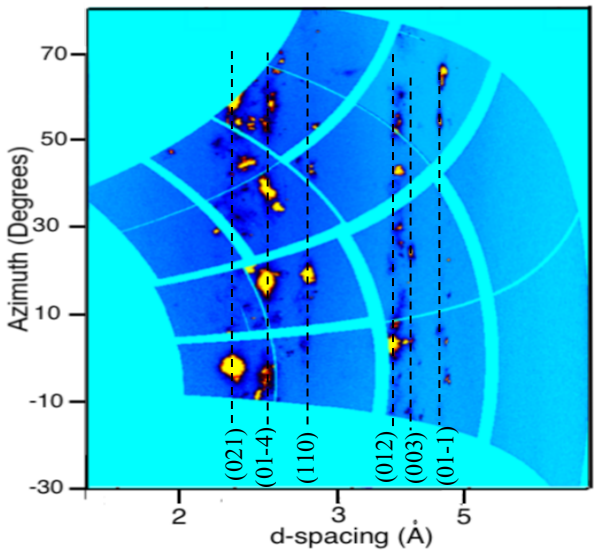

FIGURE 3. Two-dimensional X-ray diffraction image for boron carbide at a pressure of 51 GPa and time delay of 16 ns (compressed state) which is shortly before shock breakout. Sharp, circular spots arise from ambient-pressure boron carbide diffraction. Elastically compressed material exhibits peaks elongated or shifted to slightly lower d-spacing values. Other features, including most large, bright spots, are shock-compressed boron carbide as shown by dashed lines with hkl values indicated.

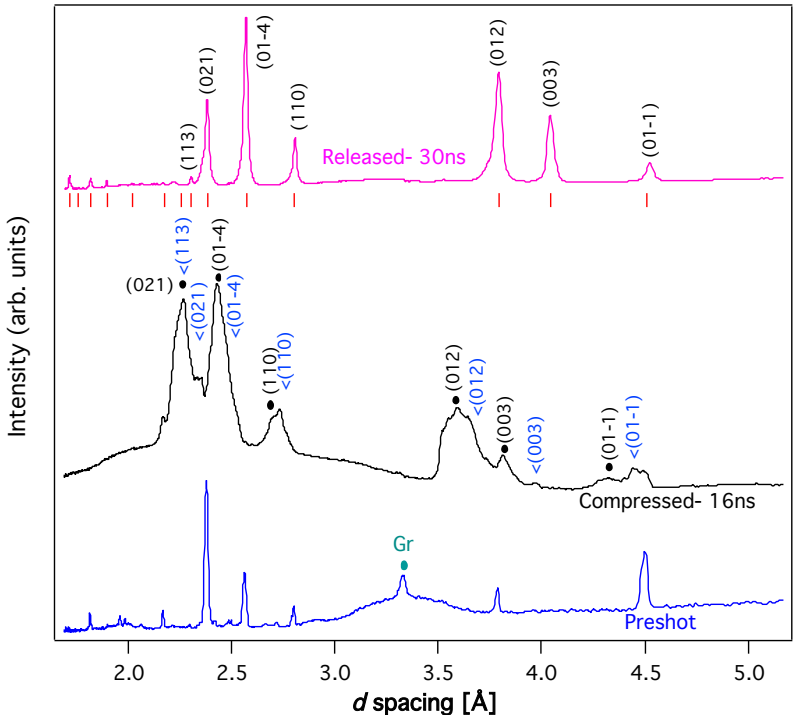

FIGURE 4. Compression and release data for boron carbide at 51 GPa. X-ray probe times after laser triggering, are listed on the right. Elastically and plastically compressed boron carbide peaks are marked with blue arrows and black dots, respectively. The uncompressed boron carbide peaks are shown by red sticks beneath the top pattern. The densities for each of the three observed states (ambient, elastic, and shock compression) are 2.52, 2.63 and 2.88 g/cm^3, respectively.

CONCLUSIONS

Boron carbide was shock compressed to 51 GPa using laser-based compression and probed by X-ray diffraction and velocity interferometry at the Materials in Extreme Conditions end-station of Linac Coherent Light Source. No evidence for a major crystallographic phase transition or disproportionation was observed along the principal Hugoniot. Densities obtained from X-ray diffraction are consistent with previous continuum shock data. Diffraction peaks from both elastically and plastically compressed boron carbide were recorded. Based on velocity interferometry measurements, the peak elastic stress for boron carbide was found to be 15.9 GPa, in agreement with previous gas-gun measurements. The samples in our study are significantly thinner, 60 μm in comparison to 2.3-9.6 mm for the gas gun, revealing no evidence for elastic precursor decay or strain rate dependence. Our starting sample contained excess carbon in the form of graphite. The graphite peaks disappeared upon compression of the sample and did not reappear upon unloading, indicating that carbon was incorporated into the structure of boron carbide behind the shock front.

ACKNOWLEDGEMENTS

We thank the staff of the Matter in Extreme Conditions end-station at the Linac Coherent Light Source and the target fabrication team at Lawrence Livermore National Laboratory for experimental assistance. Use of the Linac Coherent Light Source, SLAC National Accelerator Laboratory, is supported by the U.S. Department of Energy, Office of Science, Office of Basic Energy Sciences under Contract No. DE-AC02-76SF00515. This work was supported by the U. S. Department of Energy under awards DE- SC0016242 and DE-SC0018925.

REFERENCES

1. S. G. Savio, K. Ramanjaneyulu, V. Madhu, and T. V. Bhat, Int. J. Impact Eng. **38**, 535 (2011).
2. D. Emin, Phys. Today **40**, 56 (1987).
3. V. Domnich, S. Reynaud, R.A. Haber, and M. Chhowalla, J. Am. Ceram. Soc. **94**, 3605 (2011).
4. D. E. Grady, J. Appl. Phys. **117**, 165904 (2015).
5. P. T. Bartkowski, D. P. Dandekar, and D. J. Grove, in *Shock Compression Condens. Matter* (2002), pp. 779–782.
6. B. Nagler, B. Arnold, G. Bouchard, R. F. Boyce, R. M. Boyce, A. Callen, M. Campell, R. Curiel, E. Galtier, J. Garofoli, E. Granados, J. Hastings, G. Hays, P. Heimann, R. W. Lee, and Milathia, J. Synchrotron Radiat. **22**, 520 (2015).
7. D.E. Fratanduono, P.M. Celliers, D.G. Braun, P.A. Sterne, S. Hamel, A. Shamp, E. Zurek, K.J. Wu, A.E. Lazicki, M. Millot, and G.W. Collins, Phys. Rev. B **94**, (2016).
8. S. B. Brown, A. Hashim, A. Gleason, E. Galtier, I. Nam, Z. Xing, A. Fry, A. MacKinnon, B. Nagler, E. Granados, and H. J. Lee, Rev. Sci. Instrum. **88**, 105113 (2017).
9. G. Blaj, P. Caragiulo, G. Carini, S. Carron, A. Dragone, D. Freytag, G. Haller, P. Hart, J. Hasi, R. Herbst, S. Herrmann, C. Kenney, B. Markovic, K. Nishimura, S. Osier, J. Pines, B. Reese, J. Segal, A. Tomada, and M. Weaver, J. Synchrotron Radiat. **22**, 577 (2015).
10. D.E. Grady, J. Physiq. IV **4**, 385 (2004).
11. T. J. Vogler, W. D. Reinhart, and L. C. Chhabildas, J. Appl. Phys. **95**, 4173 (2004).
12. Y. Zhang, T. Mashimo, Y. Uemura, M. Uchino, M. Kodama, K. Shibata, K. Fukuoka, M. Kikuchi, T. Kobayashi, and T. Sekine, J. Appl. Phys. **100**, 113536 (2006).
13. W. H. Gust and E. B. Royce, J. Appl. Phys. **42**, 276 (1971).
14. S. J. Tracy, R.F. Smith, J. K. Wicks, D. E. Fratanduono, A. E. Gleason, C. A. Bolme, V. B. Prakapenka, S. Speziale, K. Appel, A. Fernandez-Pañella, H. J. Lee, A. MacKinnon, F. Tavella, J. H. Eggert, and T. S. Duffy, Phys. Rev. B **99**, 214106 (2019).
15. V. Paris, N. Frage, M.P. Dariel, and E. Zaretsky, Int. J. Impact Eng. **38**, 228 (2011).
16. P. Dera, M.H. Manghnani, A. Hushur, Y. Hu, and S. Tkachev, J. Solid State Chem. **215**, 85 (2014).
17. T. Fujii, Y. Mori, H. Hyodo, and K. Kimura, J. Phys. Conf. Ser. **215**, 012011 (2010).